# On the Theory of Corrugated Plane Surfaces*

R. S. ELLIOTT†

*Summary*—**An analysis is given of an electromagnetic system composed of a rectangular waveguide in tandem with a corrugated waveguide which feeds a flat, corrugated surface of arbitrary length terminated by a ground plane, whose length is also arbitrary. An improved procedure of field determination is used which combines Floquet's theorem and the variational principle, thus revealing an additional requirement on the corrugation geometry. Factors influencing a match at the feed mouth, and satisfactory launching of the surface wave are discussed. The degree of suppression of the feed radiation is given in db as a function of the geometry of the system. Approximate radiation patterns are derived for two cases, (a) when the system is terminated by an infinite ground plane, and (b) when the system is terminated by a finite ground plane. For the latter case, an upper bound on the tilt angle of the main beam and a lower bound on its beamwidth result from an approximate theory. For both cases, the Hansen-Woodyard endfire relation is found to provide beam sharpening even when the feed radiation is considered. The presence of higher order surface modes, their effect, and their elimination are discussed. Comparison of the theory with experiment is reasonably good.**

## Introduction

THE THEORY OF electromagnetic waves supported by corrugated conductors has been treated by many authors. In 1941 Slater[1] derived an approximate theory for wave propagation between parallel conducting plates of infinite extent, the interior surface of one of the plates being corrugated in the transverse dimension. Goldstein[2,3] extended this analysis to rectangular waveguide and Walkinshaw[4,5] applied the technique to circular waveguide. Cutler[6] appears to have been the first to demonstrate that surface waves can exist *exterior* to a single corrugated conductor. By assuming that only the dominant surface mode was present, and by matching its average surface impedance to that of the TEM modes assumed to exist between the corrugations, he succeeded in deriving approximate expressions for the phase velocity on flat and circular corrugated surfaces. By making a better approximation for the field distribution across the gaps between corrugations, Rotman[7] obtained a slight modification of Cutler's formulas.

All of these analyses were based on Floquet's theorem.[8] In 1950, Goubau[9] reviewed the work of Sommerfeld[10] pertaining to axial surface waves on cylinders and extended it to conductors with dielectric coats. Assuming a quasi-stationary field, he also showed that a conductor with a modified surface (e.g., a threaded conductor) could support an axial surface mode. Lucke[11] used a novel approach to determine the propagation constant over a single, flat corrugated surface. By considering a finite length of surface terminated by vertical conducting walls (which thus formed a resonator), he was able to get two expressions for the propagation characteristic—one in terms of the unknown electric field and the other in terms of the unknown magnetic field. The advantage of this method is that both formulations must be satisfied by the true field, so that the degree of approximation of any trial function may be gauged. The resonator method unfortunately requires the consideration of many corrugations, which makes the analysis cumbersome. By applying Floquet's theorem to Lucke's method, the analysis can be confined to a single corrugation, meanwhile retaining the desirable feature of alternative formulations.

In the next section this modified procedure is applied to a corrugated rectangular waveguide to obtain the propagation characteristics of the allowable mode configurations. The analysis is extended to a corrugated parallel plate transmission line (by letting the side walls recede to infinity) and to a single, flat corrugated surface (by then letting the top wall also recede to infinity). This affords an insight into the matching characteristics of a corrugated waveguide feeding a corrugated surface.

Radiation patterns of corrugated surfaces have been measured by the Stanford group[12] and by Ehrlich and Newkirk.[13] Discrepancies between theoretical and experimental patterns led Ehrlich to an experimental demonstration that feed radiation was contaminating the patterns and he was successful in devising techniques for reducing the effect of the feed. Theoretical support for this viewpoint will be given, together with curves of feed suppression as a function of the system geometry. It is demonstrated that by suitable design, the feed radiation can be reduced to reasonable propor-

* Revised manuscript received by PGAP, January 21, 1954. Work reported here was performed at Hughes Aircraft Company, sponsored by Air Force Cambridge Research Laboratory, Cambridge, Mass., under Contract AF 19(604)-262, and was described in Hughes Aircraft Company Technical Memorandum No. 317.

† Hughes Research and Development Labs., Culver City, Calif.

[1] J. C. Slater, "Theory of the Magnetron Oscillator," MIT Radiation Lab. Report V-5S, pp. 1–32; August, 1941.

[2] H. Goldstein, "Cavity Resonators and Waveguides Containing Periodic Elements," Ph.D. Thesis, MIT; 1943.

[3] H. Goldstein, "The Theory of Corrugated Transmission Lines and Waveguides," MIT Radiation Lab. Report 494, pp. 1–17; April, 1944.

[4] W. Walkinshaw, "Theory of Circular Corrugated Waveguide for Linear Accelerator," British TRE Report T2037; August, 1946.

[5] W. Walkinshaw, "Theoretical Design of Linear Accelerator for Electrons," *British Proc. Phys. Soc.*, vol. 345; September, 1948.

[6] C. C. Cutler, "Electromagnetic Waves Guided by Corrugated Conducting Surfaces," Bell Telephone Labs. Report MM-44-160-218; October, 1944.

[7] W. Rotman, "A study of single surface corrugated guides," PROC. I.R.E., vol. 39, pp. 952–959; August, 1951.

[8] For a discussion of Floquet's theorem the reader is referred to J. C. Slater, "Microwave Electronics," pp. 169–177, D. Van Nostrand Co., Inc., New York, N. Y.; 1950.

[9] G. Goubau, "Surface waves and their application to transmission lines," *Jour. Appl. Phys.*, vol. 21, pp. 1119–28; November, 1950.

[10] A discussion of Sommerfeld's analysis may be found in J. A. Stratton, "Electromagnetic Theory," pp. 524–537, McGraw-Hill Book Co., Inc., New York, N. Y.; 1941.

[11] Second Quarterly Progress Report, "Ridge and Corrugated Antenna Studies," Stanford Research Inst.; January, 1950.

[12] Quarterly Progress Reports 2 through 6, "Ridge and Corrugated Antenna Studies," Stanford Research Inst.; October 1949 to January 1951.

[13] M. J. Ehrlich and L. Newkirk, "Corrugated Surface Antennas," Convention Record of the I.R.E., Part 2—Antennas and Communications, pp. 18–33; 1953.

tions by some sacrifice of the match. An optimum compromise can be determined by experiment. The remaining feed radiation can be phased to improve the over-all radiation pattern. Assuming a suitable design, the radiation pattern is then contributed to chiefly by the corrugated surface and its ground plane and is characterized by an endfire main beam tilted up somewhat from the plane of the surface. An approximate theory is derived which permits an estimation of the pattern in terms of the corrugation geometry and the lengths of the corrugated surface and its ground plane. Curves of maximum tilt angle and minimum beamwidth as functions of these parameters are presented. The effect on the radiation pattern of the presence of higher order surface modes is found to be slight. Their presence would appear to be objectionable only when the corrugated surface is being used as a transmission line. They may always be suppressed simply by narrowing the teeth.

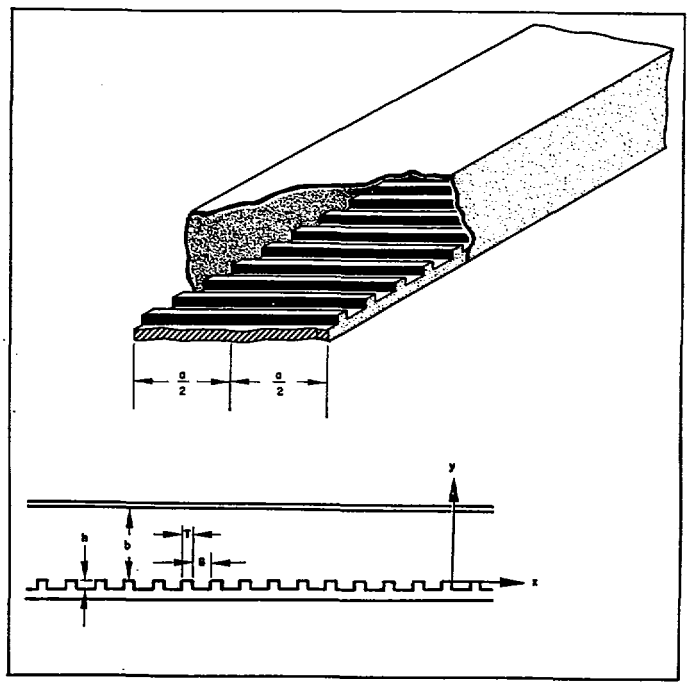


Fig. 1—Corrugated rectangular waveguide.

## The Corrugated Waveguide

As a starting point for the analysis, assume an infinitely long rectangular waveguide whose bottom wall is uniformly corrugated as shown in Fig. 1. It is desired to find the field configurations which can exist inside this structure. If $T$ is the width of a tooth and $G$ the width of a gap, the structure is periodic in units of $(T+G)$. Hence if $F(x_o, y, z)e^{j\omega t}$ is the distribution of a field component in the plane $x=x_o$ (for $O \leqq y \leqq b$, $-\lambda/2 \leqq z \leqq \frac{a}{2}$), then $F(x_o+[T+G], y, z)e^{j\omega t}=F(x_o, y, z)$ $e^{-j\beta_o(T+G)}e^{j\omega t}$ is the distribution one period further down the guide. $\beta_o$ is a complex constant whose value depends on the geometry. Since the only function which satisfies this requirement for all $x_o$ is $e^{-j\beta_o x}$ we have

$$F(x, y, z) = f(x, y, z)e^{-j\beta_o x}. \tag{1}$$

Further, $f(x, y, z)$ must be periodic in $x$ in the interval $(T+G)$ or

$$f(x, y, z) = g(y, z) \sum_{n=-\infty}^{\infty} a_n e^{-j(2\pi n x)/(T+G)}. \tag{2}$$

Thus each field component may be written in the form

$$\sum_{n=-\infty}^{\infty} g(y, z)e^{j\omega t - j\beta_n x} \tag{3}$$

in which

$$\beta_n = \beta_o + \frac{2\pi n}{T+G} \tag{4}$$

is a complex constant to be determined by the geometry. This is Floquet's theorem.

We shall assume that the structure is to be excited by a $TE_{01}$ mode incident from a tandem section of regular guide. The allowable modes in the region above the corrugations are then hybrid, characterized by the absence of an $E_z$ component, and given by

$$\begin{aligned}
E_x &= \sum_{n=-\infty}^{\infty} A_n \sinh \alpha_n(y-b)\cdot\cos\frac{\pi z}{a}\cdot e^{j(\omega t-\beta_n x)} \\
E_y &= \sum_{n=-\infty}^{\infty} \frac{j\beta_n A_n}{\alpha_n}\cosh \alpha_n(y-b)\cdot\cos\frac{\pi z}{a}\cdot e^{j(\omega t-\beta_n x)} \\
H_x &= \sum_{n=-\infty}^{\infty} \frac{-j\beta_n\pi}{j\omega\mu\alpha_n a} A_n \cosh \alpha_n(y-b)\cdot\sin\frac{\pi z}{a}\cdot e^{j(\omega t-\beta_n x)} \\
H_y &= \sum_{n=-\infty}^{\infty} \frac{\frac{\pi}{a}\cdot A_n}{j\omega\mu}\sinh \alpha_n(y-b)\cdot\sin\frac{\pi z}{a}\cdot e^{j(\omega t-\beta_n x)} \\
H_z &= \sum_{n=-\infty}^{\infty} \frac{-K^2}{j\omega\mu\alpha_n} A_n \cosh \alpha_n(y-b)\cdot\cos\frac{\pi z}{a}\cdot e^{j(\omega t-\beta_n x)}
\end{aligned} \tag{5}$$

where

$$\alpha_n = \sqrt{\beta_n^2 - K^2}, \qquad K = \sqrt{k^2 - \left(\frac{\pi}{a}\right)^2}. \tag{6}$$

With the origin of co-ordinates chosen as shown in Fig. 1, the field distribution in the gap beneath the origin may be written

$$\begin{aligned}
E_x &= -j\omega\mu\cdot B_o \sin K(y+h)\cos\frac{\pi z}{a}\cdot e^{j\omega t} \\
&\quad + \sum_{m=1}^{\infty} B_m \cos\frac{m\pi x}{G}\cdot\cos\frac{\pi z}{a}\cdot e^{j\omega t+\gamma_m y} \\
E_y &= \sum_{m=1}^{\infty} \frac{m\pi}{\gamma_m G} B_m \sin\frac{m\pi x}{G}\cos\frac{\pi z}{a}\cdot e^{j\omega t+\gamma_m y} \\
H_x &= -\sum_{m=1}^{\infty} \frac{\pi}{j\omega\mu\gamma_m a}\cdot\frac{m\pi}{G}\cdot B_m\cdot\sin\frac{m\pi x}{G}\cdot\sin\frac{\pi z}{a}\cdot e^{j\omega t+\gamma_m y} \\
H_y &= -\frac{\pi}{a}\cdot B_o\cdot\sin K(y+h)\cdot\sin\frac{\pi z}{a}\cdot e^{j\omega t}
\end{aligned}$$

$$+\sum_{m=1}^{\infty}\frac{1}{j\omega\mu}\cdot\frac{\pi}{a}\cdot B_m\cdot\cos\frac{m\pi x}{G}\cdot\sin\frac{\pi z}{a}\cdot e^{j\omega t+\gamma_m y}$$

$$H_z=-KB_o\cos K(y+h)\cdot\cos\frac{\pi z}{a}\cdot e^{j\omega t}$$

$$-\sum_{m=1}^{\infty}\frac{K^2}{j\omega\mu\gamma_m}B_m\cos\frac{m\pi x}{G}\cdot\cos\frac{\pi z}{a}\cdot e^{j\omega t+\gamma_m y} \tag{7}$$

in which

$$\sqrt{m}=\sqrt{\left(\frac{m\pi}{G}\right)^2-K^2}. \tag{8}$$

Implicit in (7) is the concept that each slot is a short-circuited waveguide of length $h$. The $m$ series represents that combination of $TM$ and $TE$ modes, all beyond cutoff, which together satisfy the requirement that $E_z\equiv O$. It is assumed that the slot width $G$ is so small compared to the free space wavelength that all of these modes are attenuated to a negligible amplitude before they reach the bottom of the slot and hence have no reflected component. The one propagating mode is represented by the standing wave terms, written separately in (7). Thus $K$ and $\sqrt{m}$, given by (8), are positive real quantities determined solely by the geometry.

Since the tangential fields must be continuous across the boundary between the two regions, that is, across the plane $y=O$, one may equate the integrals

$$\int_{-a/2}^{+a/2}\int_0^{G+T}\vec{E}_1\times\vec{H}_1^*\cdot\vec{u}_y dxdz$$

$$\equiv\int_{-a/2}^{+a/2}\int_0^{G}\vec{\mathcal{E}}_1\times\vec{\mathcal{H}}_1^*\cdot\vec{u}_y dxdz \tag{9}$$

in which $\vec{E}_1$, $\vec{H}_1$ are the unknown fields expressed in terms of (5) and $\vec{\mathcal{E}}_1$, $\vec{\mathcal{H}}_1$ are the unknown fields expressed in terms of (7). All terms of the integrands of (9) contain $z$ only in the factor $\cos \pi z/a$. Hence (9) reduces to

$$\int_0^{G+T}EH^*dx=\int_0^{G}\mathcal{E}\mathcal{H}^*dx \tag{10}$$

where

$$E=-\sum_{n=-\infty}^{\infty}A_n\sinh\alpha_n b\cdot e^{j(\omega t-\beta_n x)} \tag{11a}$$

$$H=-\sum_{n=-\infty}^{\infty}\frac{K^2}{j\omega\mu\alpha_n}A_n\cosh\alpha_n b\cdot e^{j(\omega t-\beta_n x)} \tag{11b}$$

$$\mathcal{E}=-j\omega\mu B_o\sin Kh\cdot e^{j\omega t}+\sum_{m=1}^{\infty}B_m\cos\frac{m\pi x}{G}\cdot e^{j\omega t} \tag{11c}$$

$$\mathcal{H}=-KB_o\cos Kh\cdot e^{j\omega t}-\sum_{m=1}^{\infty}\frac{K^2}{j\omega\mu\gamma_m}\cdot B_m\cos\frac{m\pi x}{G}\cdot e^{j\omega t} \tag{11d}$$

and

$$E\equiv\mathcal{E},\qquad H\equiv\mathcal{H}. \tag{12}$$

The Fourier coefficients $A_n$ and $B_m$ may be expressed in terms of integrals of the unknown electric field, i.e.,

$$A_n^*=-\frac{1}{(G+T)\sinh\alpha_n b}\int_0^{G+T}E^*e^{j(\omega t-\beta_n x)}dx \tag{13}$$

$$B_o^*=\frac{1}{j\omega\mu G\sin Kh}\int_0^{G}\mathcal{E}^*e^{j\omega t}dx \tag{14}$$

$$B_m^*=\frac{2}{G}\int_0^{G}\mathcal{E}^*\cos\frac{m\pi x}{G}\cdot e^{j\omega t}dx \tag{15}$$

and when these relations are substituted in (11b) and (11d) the magnetic field is given in terms of the electric field. Upon inserting the resulting expressions for the magnetic field in (10), making use of (12), and rearranging terms, one obtains

$$\cot Kh=\frac{\sum_{n=-\infty}^{\infty}\frac{G}{G+T}\cdot\frac{K}{\alpha_n}\cdot\coth\alpha_n b\int_0^{G+T}Ee^{j\beta_n x}dx\int_0^{G+T}E^*e^{-j\beta_n x}dx+\sum_{m=1}^{\infty}\frac{2K}{\gamma_m}\int_0^{G}E\cos\frac{m\pi x}{G}dx\int_0^{G}E^*\cos\frac{m\pi x}{G}dx}{\int_0^{G}Edx\int_0^{G}E^*dx} \tag{16}$$

By a similar procedure, (12) can be expressed entirely in terms of the unknown field $H$, giving

$$\frac{1}{\cot Kh}=\frac{\sum_{n=-\infty}^{\infty}\frac{G}{G+T}\cdot\frac{\alpha_n}{K}\cdot\tanh\alpha_n b\int_0^{G+T}He^{j\beta_n x}dx\int_0^{G+T}H^*e^{-j\beta_n x}dx+\sum_{m=1}^{\infty}\frac{2\gamma_m}{K}\int_0^{G}H\cos\frac{m\pi x}{G}dx\int_0^{G}H^*\cos\frac{m\pi x}{G}dx}{\int_0^{G}Hdx\int_0^{G}H^*dx} \tag{17}$$

Equations (16) and (17) are suggestive of Schwinger's variational form but investigation discloses that only (17) is stationary about the true fields.[14] However, both must be *satisfied* by the true fields and from this fact

[14] R. S. Elliott, "On the Theory of Corrugated Plane Surfaces," Hughes Research and Development Labs., Technical Memorandum No. 317; October, 1953. (Revised.)

one can derive useful information. To see how good an approximation the fundamental mode is, we insert the trial function $E=-A_0 \sinh \alpha_o b \cdot e^{j(\omega t-\beta_o x)}$ in (16) and obtain the asymptotic formula

$$\cot Kh = \frac{G+T}{G}\cdot\frac{K}{\alpha_o}\coth \alpha_o b \tag{18}$$

as $G+T\to O$. Similarly, when the companion trial function

$$H = -\frac{K^2}{j\omega\mu\alpha_o} A_o \cosh \alpha_o b \cdot e^{j(\omega t-\beta_o x)}$$

is inserted in (17), the asymptotic formula

$$\cot Kh = \frac{G}{G+T}\cdot\frac{K}{\alpha_o}\cdot\coth \alpha_o b \tag{19}$$

results when $G+T\to O$. Previous work by the Stanford group on a similar problem[11] indicates that these formulas are good representations for $(\lambda_o/G+T)\geqq 10$.

It is interesting to note that only for $T=O$ are the two formulas the same. This is reasonable when one recalls that $E_{\tan}\equiv O$ over each tooth and the trial function used to obtain (18) does not satisfy this requirement if $T>O$. Hence, we conclude that only if (a) the number of corrugations/wavelength is large, and (b) tooth width/gap width is small, does the field distribution above the corrugations consist essentially of the fundamental mode. Point (b) seems previously to have been overlooked and it can have important bearing on the impedance concept when corrugated surfaces are used as transmission lines. This shall be discussed further in a later section.

The question still remains as to which formula, (18) or (19), is more accurate when $T>O$. One would suspect (19) is, because of its stationary character, and because of the severe requirement on $E_{\tan}$. Support for this belief arises when any more general trial function is substituted in (16) and (17). The variation in (16) is always greater than the corresponding variation in (17).

Henceforth we shall assume that there are at least ten corrugations per wavelength and that the teeth are narrow compared to the gaps. Then to a good approximation the field above the corrugations is given by

$$E_x = A_o \sinh \alpha_o(y-b)\cdot\cos\frac{\pi z}{a}\cdot e^{j(\omega t-\beta_o x)}$$

$$E_y = \frac{j\beta_o}{\alpha_o} A_o \cosh \alpha_o(y-b)\cdot\cos\frac{\pi z}{a}\cdot e^{j(\omega t-\beta_o x)}$$

$$H_x = -\frac{j\beta_o\pi}{j\omega\mu\alpha_o a} A_o \cosh \alpha_o(y-b)\cdot\sin\frac{\pi z}{a}\cdot e^{j(\omega t-\beta_o x)}$$

$$H_y = \frac{\pi}{j\omega\mu a} A_o \sinh \alpha_o(y-b)\cdot\sin\frac{\pi z}{a}\cdot e^{j(\omega t-\beta_o x)}$$

$$H_z = -\frac{K^2}{j\omega\mu\alpha_o} A_o \cosh \alpha_o(y-b)\cdot\cos\frac{\pi z}{a}\cdot e^{j(\omega t-\beta_o x)}$$

$$\alpha_o = \sqrt{\beta_o^2 - K^2}$$

$$\cot Kh = \frac{G}{G+T}\cdot\frac{K}{\alpha_o}\coth \alpha_o b$$

$$K = \sqrt{k^2-\left(\frac{\pi}{a}\right)^2}. \tag{20}$$

We notice that if $O\leqq Kh\leqq(\pi/2)$ then $\beta_o$ and $\alpha_o$ are both real and $\beta_o>K$ so that wave propagation is slower than it would be in uncorrugated guide.

If the side walls are allowed to recede to infinity, the solution for a corrugated parallel plate transmission line is obtained. Namely,

$$E_x = A_o \sinh \alpha_o(y-b)e^{j(\omega t-\beta_o x)}$$

$$E_y = \frac{j\beta_o}{\alpha_o} A_o \cosh \alpha_o(y-b)e^{j(\omega t-\beta_o x)}$$

$$H_z = \frac{j\omega\epsilon}{\alpha_o} A_o \cosh \alpha_o(y-b)e^{j(\omega t-\beta_o x)}$$

$$\alpha_o = \sqrt{\beta_o^2 - k^2}$$

$$\cot kh = \frac{G}{G+T}\cdot\frac{\coth \alpha_o b}{\sqrt{(\beta_o/k)^2-1}}. \tag{21}$$

If the spacing $b$ becomes indefinitely large, the solution for a single flat corrugated surface results:

$$E_x = Ae^{j\omega t-j\beta_o x-\alpha_o y}$$

$$E_y = -\frac{j\beta_o}{\alpha_o} Ae^{j\omega t-j\beta_o x-\alpha_o y}$$

$$H_z = \frac{-j\omega\epsilon}{\alpha_o} Ae^{j\omega t-j\beta_o x-\alpha_o y}$$

$$\alpha_o = \sqrt{\beta_o^2 - k^2}$$

$$\cot kh = \frac{G}{G+T}\cdot\frac{1}{\sqrt{(\beta_o/k)^2-1}}$$

in which

$$A = \lim_{b\to\infty}\left[-\frac{A_o}{2}e^{\alpha_o b}\right]. \tag{22}$$

Thus we conclude that if the side and top walls of a corrugated waveguide are gradually flared out and then terminated, a surface wave may be satisfactorily launched on the extended bottom wall with the expectation of a good match. If at the other end of the corrugated waveguide the depth of corrugations is gradually tapered to zero, a good match to regular guide can be achieved[13] and the resulting system can be efficiently excited by a $TE_{01}$ mode.[15]

## Radiation from Corrugated Surfaces

A problem of considerable practical interest is the computation of the radiation pattern of the system of

[15] As with any horn, there are space limitations to such a system and for wide surfaces, line feeds (such as pill boxes, hog horns, etc.) are more desirable. In such cases, flaring of the top wall is still helpful to the match.

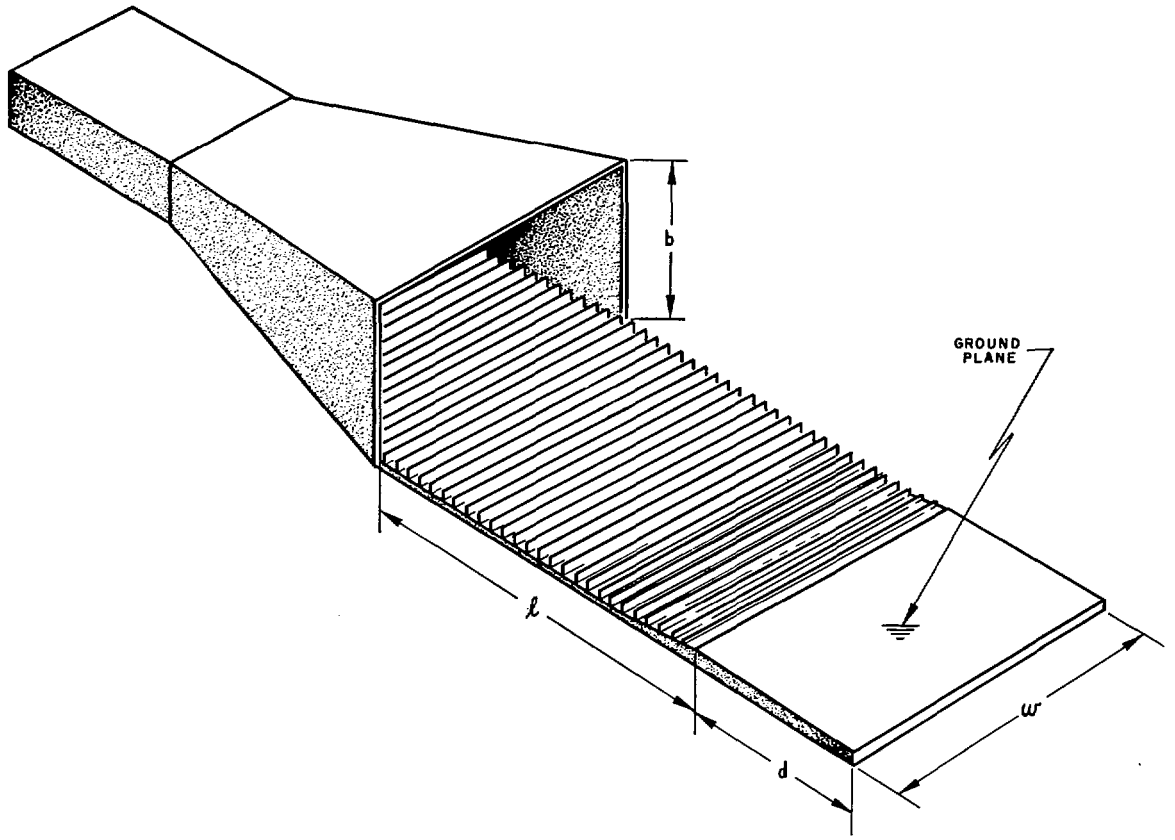


Fig. 2—Corrugated surface antenna.

Fig. 2. We shall assume all the requirements for a good match are met, i.e., tapered corrugations in the wave guide and gentle flare angles for the horn to a large aperture $b \times w$. It is then reasonable to expect that most of the power incident in a $TE_{01}$ mode is transformed to a surface mode as given by (22).

Since the chief effect of the finite width $w$ is to alter the horizontal beamwidth, we shall infer the solution of this problem from the similar but simpler problem of an infinitely wide parallel plate transmission line whose lower plate is corrugated and extended out to form a single surface, as shown in Fig. 3. For the present, we shall assume the surface to be terminated by an infinite ground plane, deferring to the next section a discussion of the effect of a finite ground plane. The radiation pattern of the system of Fig. 3 is contributed to by the secondary source distribution across the mouth of the aperture, the current distribution in the corrugated section of length $l$, and the current distribution in the infinite ground plane. (The assumption of a good match implies that the currents which leak back over the outside of the upper plate are negligible. If $f \ll l$ it may be ignored. If not, the effective length $l'$ can be taken as some reasonable compromise, such as $l' = l + \frac{1}{2}f$.)

Lucke has shown[16] that for $f = O$ the reflection coefficient for a surface wave of the form (22), incident at the junction of the corrugated surface and its infinite ground plane, is given in magnitude by

$$|R| = \frac{\beta_o - k}{\beta_o} \cdot \tag{23}$$

We shall see shortly that maximum gain results for the corrugated surface of Fig. 3 if $(\beta_o - k)l = \pi$ (the Hansen-Woodyard relation). Hence for practical systems $\beta_o/k - 1$ is small and likewise $|R|$ is small. The tapered section $f$ tends to reduce $|R|$ still further so we shall assume no reflection at all.

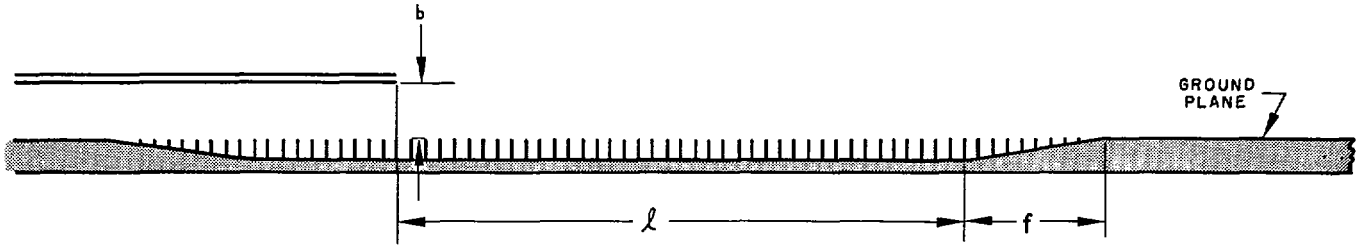


Fig. 3—Simplified antenna system.

[16] Third Quarterly Progress Report, "Ridge and Corrugated Antenna Studies," Stanford Research Inst.; April, 1950.

The field distribution over the corrugated surface is then given by (22). If this field is terminated by the electric and magnetic current sheets

$$\vec{J} = -\vec{u}_x \frac{j\omega\epsilon}{\alpha_o^s} A e^{j(\omega t-\beta_o^s x)} \tag{24}$$

$$\vec{J}_m = \vec{u}_z A e^{j(\omega t-\beta_o^s x)} \tag{25}$$

the corrugated surface may be removed and the ground plane extended back to the mouth of the feed. The effect of the ground plane can then be accounted for by the method of images.

Referring to (21), the field at the mouth of the feed can be terminated by the sheets

$$\vec{J} = -\vec{u}_y \frac{j\omega\epsilon}{\alpha_o^F} A_o \cosh \alpha_o^F(y-b) e^{j(\omega t-\beta_o^F x_o)} \tag{26}$$

$$\vec{J}_m = -\vec{u}_z \frac{j\beta_o^F}{\alpha_o^F} A_o \cosh \alpha_o^F(y-b) e^{j(\omega t-\beta_o^F x_o)} \tag{27}$$

in which $x_o$ is the $x$-co-ordinate of the aperture. (The superscripts $s$ and $F$ are employed as mnemonic devices for the surface and feed respectively.) The images of (24)–(27) are

$$\vec{J} = \vec{u}_x \frac{j\omega\epsilon}{\alpha_o^s} A e^{j(\omega t-\beta_o^s x)} \tag{24a}$$

$$\vec{J}_m = \vec{u}_z A e^{j(\omega t-\beta_o^s x)} \tag{25a}$$

$$\vec{J} = -\vec{u}_y \frac{j\omega\epsilon}{\alpha_o^F} A_o \cosh \alpha_o^F(|y|-b) e^{j(\omega t-\beta_o^F x_o)} \tag{26a}$$

$$\vec{J}_m = -\vec{u}_z \frac{j\beta_o^F}{\alpha_o^F} A_o \cosh \alpha_o^F(|y|-b) e^{j(\omega t-\beta_o^F x_o)} \tag{27a}$$

so that the original system is equivalent to a magnetic current sheet

$$\vec{J}_m = \vec{U}_z 2A e^{j(\omega t-\beta_o^s x)} \tag{28}$$

occupying the same position as the corrugated surface, and a double sheet

$$\vec{J} = -\vec{u}_y \frac{j\omega\epsilon}{\alpha_o^F} A_o \cosh \alpha_o^F(|y|-b) e^{j(\omega t-\beta_o^F x_o)} \tag{29}$$

$$\vec{J}_m = -\vec{u}_z \frac{f\beta_o^F}{\alpha_o^F} A_o \cosh \alpha_o^F(|y|-b) e^{j(\omega t-\beta_o^F x_o)} \tag{30}$$

extending from $-b$ to $+b$ in the plane of the feed mouth ($x=x_o$).

The radiation patterns of these sources are

$$H_z^s = -\frac{\omega\epsilon}{2} lA\sqrt{\frac{2}{\pi k\rho_0}} \cdot e^{j(\omega t-k\rho_0+\pi/4)} \frac{\sin \frac{\pi l}{\lambda}\left[\frac{\beta_o^s}{k}-\cos\theta\right]}{\frac{\pi l}{\lambda}\left[\frac{\beta_o^s}{k}-\cos\theta\right]} = \tag{31}$$

$$H_z^F = j\omega\epsilon A_o \frac{\beta_o^F + k\cos\theta}{2\alpha_o^F}\sqrt{\frac{2}{\pi k\rho_o}} \cdot e^{j(\omega t-k\rho_o+\pi/4)} e^{j(\pi l/\lambda)(\beta_o^F/k-\cos\theta)} \times \frac{k\sin\theta\cdot\sin[kb\sin\theta] + \alpha_o^F \sinh \alpha_o^F b}{(\alpha_o^F)^2 + k^2\sin^2\theta} \tag{32}$$

in which the center of the corrugated surface has been chosen as origin (making $x_o=-l/2$). The corrugated surface is seen to give a conventional endfire pattern which can be maximized by setting

$$(\beta_o^s - k)l = \pi. \tag{33}$$

This is the Hansen-Woodyard relation mentioned previously.

Although there is considerable turbulence in the region of the mouth, if the guide and surface modes are extrapolated to the position $x=-l/2$, we can write

$$\frac{-A_o \sinh \alpha_o^F b\cdot e^{j(\beta_o^F l)/2}}{A e^{j(\beta_o^s l)/2}} = Ce^{i\psi} \tag{34}$$

in which $C$ and $\psi$ are positive real numbers which depend on the corrugation geometry and the mouth height, $b$, but *not* on length of corrugated surface, $l$, since it is assumed there are no reflections. The quantity

$$\frac{C^2}{\sinh^2 \alpha_o^F b} = \left|\frac{A_o}{A}\right|^2 \tag{35}$$

can be found by equating the power in the guide and surface modes, which gives

$$\left|\frac{A_o}{A}\right|^2 = \frac{\beta_o^s}{\beta_o^F}\left(\frac{\alpha_o^F}{\alpha_o^s}\right)^3 \frac{1}{\alpha_o^F b + \sinh \alpha_o^F b\cdot\cosh \alpha_o^F b}. \tag{36}$$

Both fields (31) and (32) have their maxima in the direction $\theta=0$ degrees. Making the substitutions (33) and (34), the ratio of these maxima is

$$\frac{H_z^s}{H_z^F} = -\frac{2l(\beta_o^F - k)}{\pi C e^{i\psi}} \tag{37}$$

and the corresponding power ratio is

$$\frac{P^s}{P^F}(\theta = 0°) = \frac{4l^2(\beta_o^F - k)^2}{\pi^2 C^2}. \tag{38}$$

This relationship is plotted in Fig. 4 for several lengths of corrugated surface. It is seen that the mouth must be made quite small to effect satisfactory feed suppression. This is going contrary to the requirements for a good match, and the analysis breaks down when the match is poor enough that it is no longer proper to equate the powers in the two modes. Hence, some optimum height $b$ exists, which for practical systems probably will not yield more than 10 to 15 db of suppression. This optimum height will be a function of $\beta_o^s$ and $l$ and can best be determined by experiment.

It is observed from (37) that if $\psi$ is small (which seems reasonable) the two fields are essentially out of phase in the forward direction. Since the feed pattern is broad, this tends to sharpen the main beam. As an illustration of this, Fig. 5 shows the experimental pattern of a 7.33λ corrugated surface as measured by Ehrlich. $\beta_o^s$ was adjusted to give maximum gain, i.e., $(\beta_o^s-k)l=\pi$. For

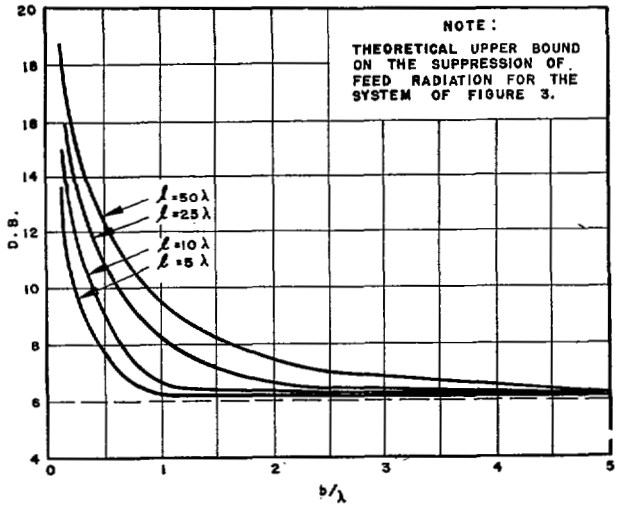


Fig. 4—Feed suppression in db.

comparison, the theoretical patterns for the corrugated surface alone, and for the surface plus feed with $\psi = O$, $\pi$ are plotted. It is seen that the case $\psi = O$ corresponds most closely to experiment. Thus it is wise to use the Hansen-Woodyard relation even when the feed radiation is considered, for the phasing is then proper to provide additional beam sharpening. This will also be seen to be true in the presence of finite ground planes.

### The Effect of a Finite Ground Plane

Thus far the corrugated surface has been assumed to be terminated by an infinite ground plane which permits the use of the image principle and greatly simplifies the analysis. A reasonable approximation to the pattern for the case of a finite ground plane can be obtained by assuming the dominant mode to be present over the corrugations and by assuming the same current distribution to exist in the finite ground plane as would exist in the same portion of an infinite ground plane.

For the case of no ground plane at all, this implies the radiation pattern arises essentially from the double sheet (24) and (25). (We assume feed radiation is sufficiently suppressed as to be only a minor perturbation on results following.) This radiation pattern is given by

$$H_z = -(\alpha_o{}^s + jk\sin\theta)\,\frac{\omega\epsilon l A}{4\alpha_o{}^s}\sqrt{\frac{2}{\pi k\rho_o}}\,e^{j(\omega t - k\rho_o + \pi/4)} \cdot \frac{\sin\frac{\pi l}{\lambda}\left[\frac{\beta_o{}^s}{k} - \cos\theta\right]}{\frac{\pi l}{\lambda}\cdot\left[\frac{\beta_o{}^s}{k} - \cos\theta\right]}; \qquad 0 < \theta < \pi \tag{39}$$

and is an approximation which is valid only for $(\beta_o{}^s - k)l$ small. A plot of (39) is characterized by a main beam tilted up from the endfire position and slightly broadened with respect to the infinite ground plane case. These results are consistent with experiment. The tilt angle of the main beam is given by

$$\frac{\tan\frac{\pi l}{\lambda}\left[\frac{\beta_o{}^s}{k} - \cos\theta_T\right]}{\frac{\pi l}{\lambda}\cdot\left[\frac{\beta_o{}^s}{k} - \cos\theta_T\right]} = 1 + \frac{k}{\beta_o{}^s}\cos\theta_T. \tag{40}$$

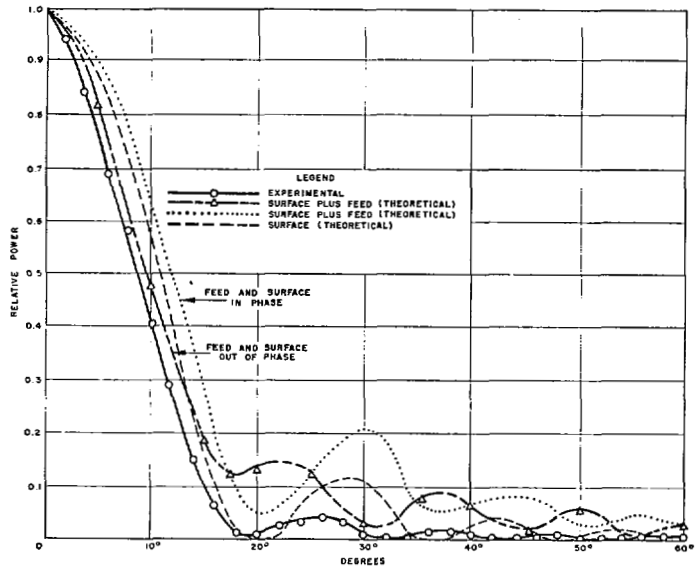


Fig. 5—Theoretical and experimental radiation patterns for a corrugated surface of length 7.33λ excited by a waveguide.

This tilt angle is a decreasing function of $\beta_o{}^s/k$ for all lengths $l$ and thus has an upper bound for $\beta_o{}^s/k = 1$. This is fortunate, for the approximation is most accurate for this minimum value of $\beta_o{}^s/k$. A plot of the upper bound is shown in Fig. 6, on following page.

To see what happens as ground plane is added, we first must find the current distribution in the infinite ground plane. Using the source system (28), we find

$$J_x = H_z = -\frac{\omega\epsilon A}{2}\,e^{j\omega t}\int_{-l/2}^{l/2} H_o{}^{(2)}\left[k(x - x')\right]e^{-j\beta_o{}^s x'}dx' \qquad \frac{l}{2} \leqq x < \infty. \tag{41}$$

This may be converted to

$$J_x = -\frac{\omega\epsilon A}{2k}\,e^{j(\omega t - \beta_o{}^s x)}\int_{k(x-l/2)}^{k(x+l/2)} H_o{}^{(2)}(u)\,e^{j(\beta_o{}^s/k)u}du \tag{42}$$

in which $u = k(x - x')$. When the Hansen-Woodyard relation, $(\beta_o{}^s - k)l = \pi$, is satisfied, the phase change of the integrand of (42) over the interval $k(x - l/2) \leqq u \leqq k(x + l/2)$ is approximately $\pi$ radians for all $x$. Thus the integrated error accruing from the substitution

$$H_o{}^{(2)}(u) = \sqrt{\frac{2}{\pi u}}\,e^{-iu}e^{j(\pi/4)} \tag{43}$$

is negligible for all $x$ in the range

$$\frac{\lambda}{2} \leqq x - \frac{l}{2} < \infty. \tag{44}$$

Then

$$J_x = -\frac{\omega\epsilon A}{k\sqrt{2\pi}}\,e^{j(\omega t - \beta_o{}^s z + \pi/4)}\int_{k(x-l/2)}^{k(x+l/2)} \frac{e^{j(\beta_o{}^s/k - 1)u}}{\sqrt{u}}\,du \qquad \frac{l}{2} + \frac{\lambda}{2} \leqq x < \infty. \tag{45}$$

Equation (45) may be solved in terms of Fresnel integrals through the substitution

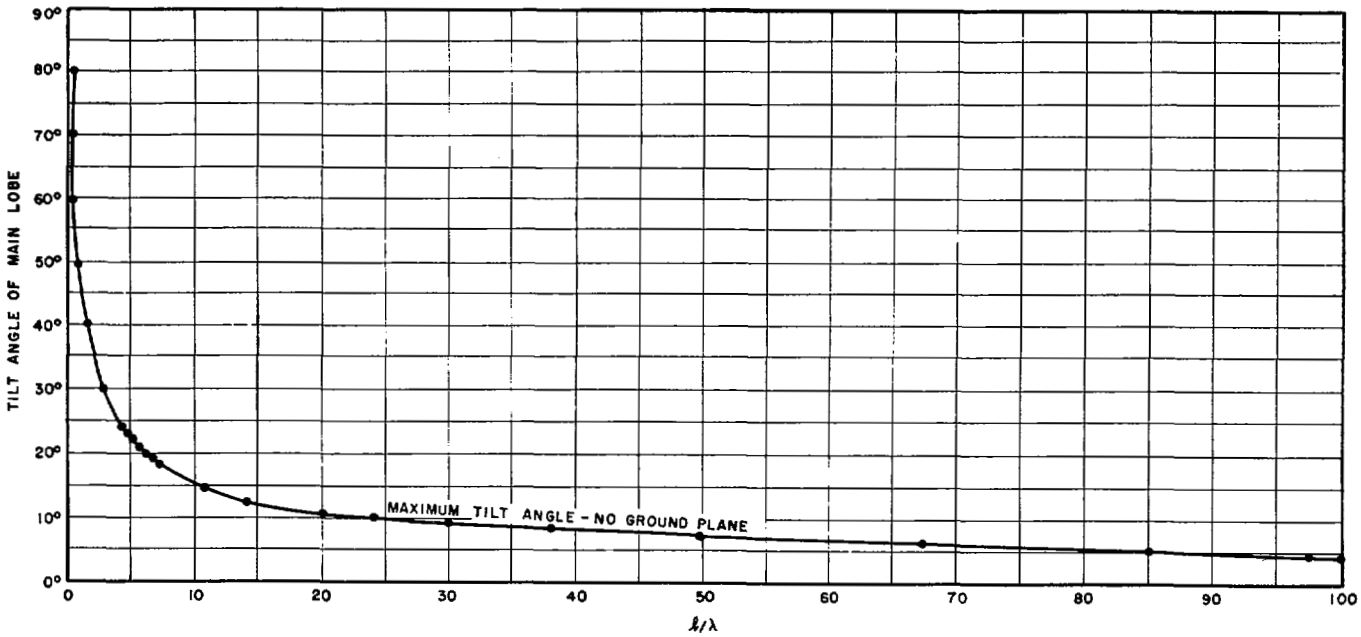


Fig. 6—Theoretical upper bound on the main beam-tilt angle for the radiation pattern of a flat corrugated surface with no ground plane.

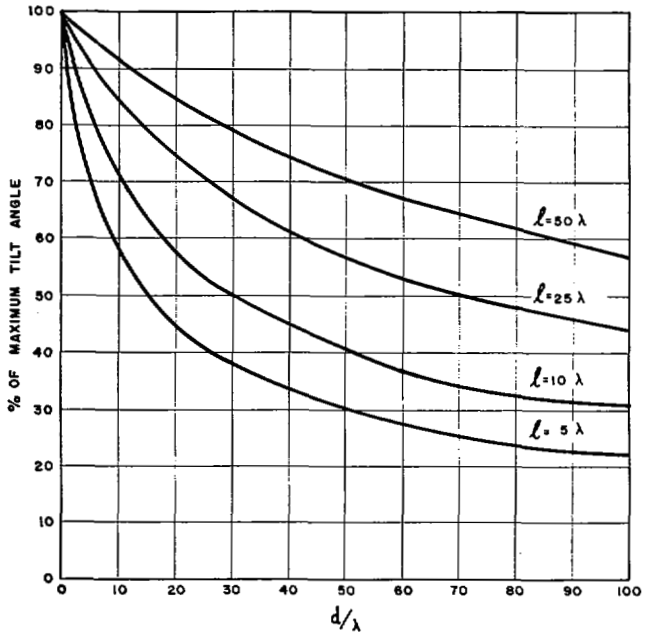


Fig. 7—Theoretical upper bound on the main beam-tilt angle of the radiation pattern for a flat corrugated surface as a function of the lengths of the surface and its ground plane.

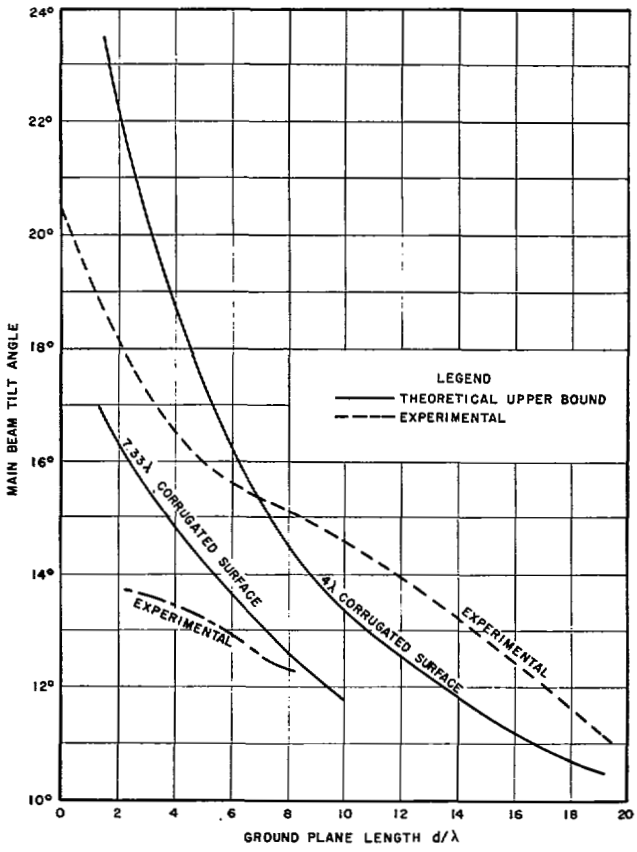


Fig. 8—Comparison between theory and experiment for two corrugated surfaces obeying the Hansen-Woodyard relation, one 7.33λ long and the other 4λ long.

$$\sqrt{\frac{\pi}{2}}\,v = \sqrt{\left(\frac{\beta_o{}^s}{k} - 1\right)u} \tag{46}$$

with the result

$$J_x = -\frac{\omega\epsilon A}{\sqrt{k(\beta_o{}^s - k)}} \cdot e^{j(\omega t - \beta_o{}^s x + \pi/4)}\left[C(v) + jS(v)\right]_{\sqrt{2(\beta_o{}^s - k)x - \pi}}^{\sqrt{2(\beta_o{}^s - k)x + \pi}}$$

$$\frac{l}{2} + \frac{\lambda}{2} \leqq x < \infty. \tag{47}$$

Since the value of $J_x$ is also known at $x = l/2$, the current distribution in the intervening half-wavelength can be inferred by extrapolation. Equation (47) indicates that for a given $x$, the current density is a decreasing function of $\beta_o{}^s/k$. Thus for a finite ground plane of length $d$, with the assumed current distribution (47), the larger the value of $\beta_o{}^s/k$, the smaller the end disturbance and the smaller the tilt angle. Therefore the tilt angle is a decreasing function of $d$ for all $\beta_o{}^s/k$, with the rate of decrease least for $\beta_o{}^s/k = 1$. But for the case $\beta_o{}^s/k = 1$, the corrugated surface of length $l$, and its ground plane of

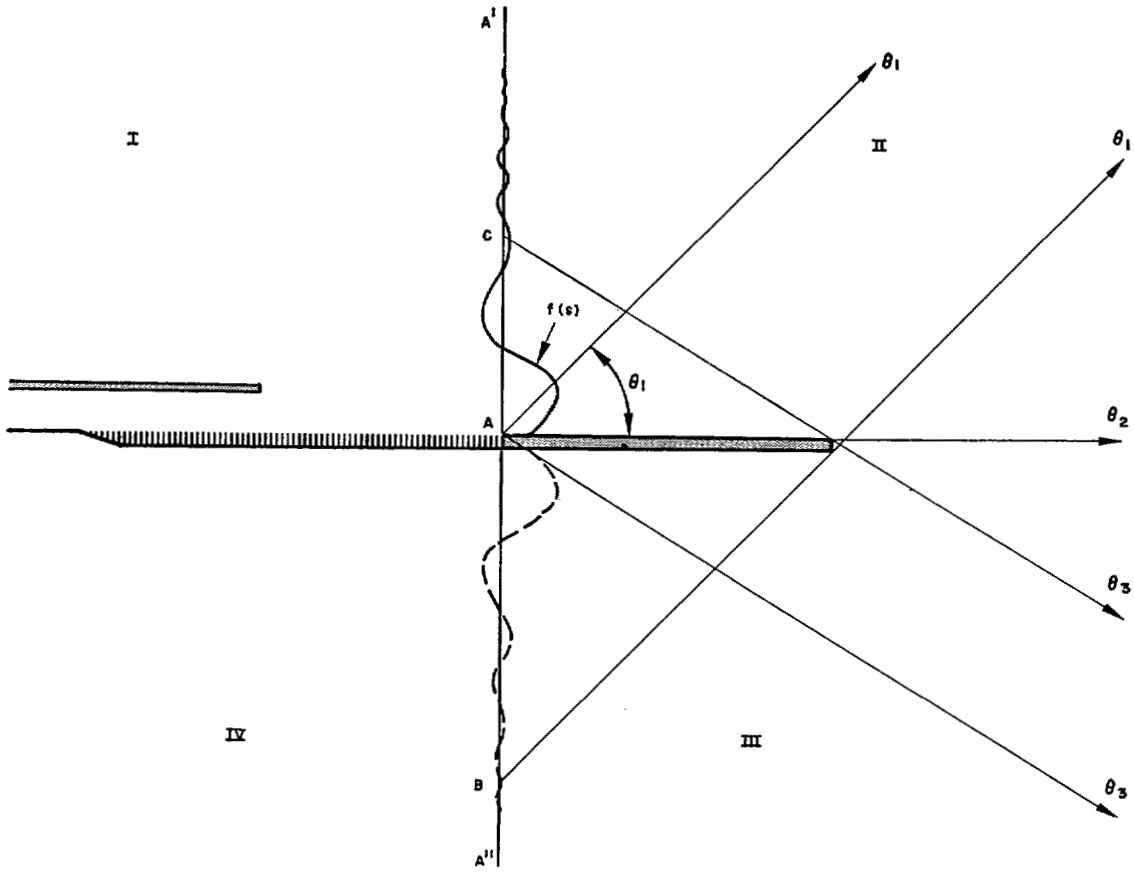


Fig. 9—Geometrical optics formulation.

length $d$ are electrically indistinguishable, and Fig. 6 becomes the upper bound when $(l+d)/\lambda$ is substituted for $l/\lambda$ as the abscissa scale. This information can be plotted in an alternative way as shown in Fig. 7, left.

To check this theory, a series of ground planes of length $0\lambda$ to $19\lambda$ were added to a $4\lambda$ corrugated surface and the tilt angles measured. In a second experiment, ground planes ranging from $2\lambda$ to $8\lambda$ were attached to a $7.33\lambda$ corrugated surface and the measurements repeated. The results are shown in Fig. 8, page 78. The agreement with theory is fair, with the greatest departure occurring for long ground planes.

A satisfactory picture of the general nature of the four-quadrant radiation pattern can be gleaned from a geometrical optics argument.

Referring to Fig. 9, (shown above) if we neglect the feed radiation and assume that the current distribution in the ground plane does not radiate in the backward direction, the radiation field along the half-plane $A-A'$ is given by (39) and if this field is terminated by the proper double sheet the radiation field in quadrants II, III, and IV is approximately determined by this double sheet in the presence of the ground plane as an obstacle. The amplitude distribution of the source system along $A-A'$ is suggested by the curve $f(s)$ and serves to explain many of the features of the pattern.

For an angle $\theta_1$ in quadrant II, the radiation is computed from the sources along $A-A'$ plus the image sources from $B$ to $A$. As $\theta_1$ approaches 90 degrees, the radiation approaches the value computed for an infinite ground plane, and throughout quadrant I we assume that the radiation pattern does correspond to this infinite case. As $\theta_1$ approaches 0 degrees, fewer of the image sources contribute, and in the position $\theta_2$, the field strength is down to one-half the value found for the infinite case. At any angle $\theta_1$, the radiation approaches more nearly to the infinite case as the ground plane is lengthened.

For an angle $\theta_3$ in quadrant III, only the sources from $C$ to $A'$ contribute and as $\theta_3$ approaches $-90$ degrees, field decreases to zero, oscillating slightly as changing source system phases in and out. Under this geometrical argument, no energy is found in quadrant IV.

Using the above model, a sketchy picture of the radiation pattern may be synthesized as follows: For the lengths $l$ and $d$ of surface and ground plane being considered, determine from Figs. 6 and 7 the approximate tilt angle, $\theta_T$, of the main beam. Use the field distribution (31) for the region $\theta_T \leqq \theta \leqq 180$ degrees, assuming the null positions are undisturbed. For the region $-90$ degrees $\leqq \theta \leqq \theta_T$ sketch in a smoothly decreasing field approximately 6 db down at $\theta = 0$ degrees. Result for a $7.33\lambda$ surface with a $\frac{1}{2}\lambda$ ground plane is in Fig. 10, page 80. This pattern agrees in its general shape with measured patterns, two examples of which are given in Fig. 11, on page 81.

## Beamwidth

The geometrical optics picture just outlined suggests that for a corrugated surface of given length "$l$," as the ground plane length "$d$" is increased, the main beam not

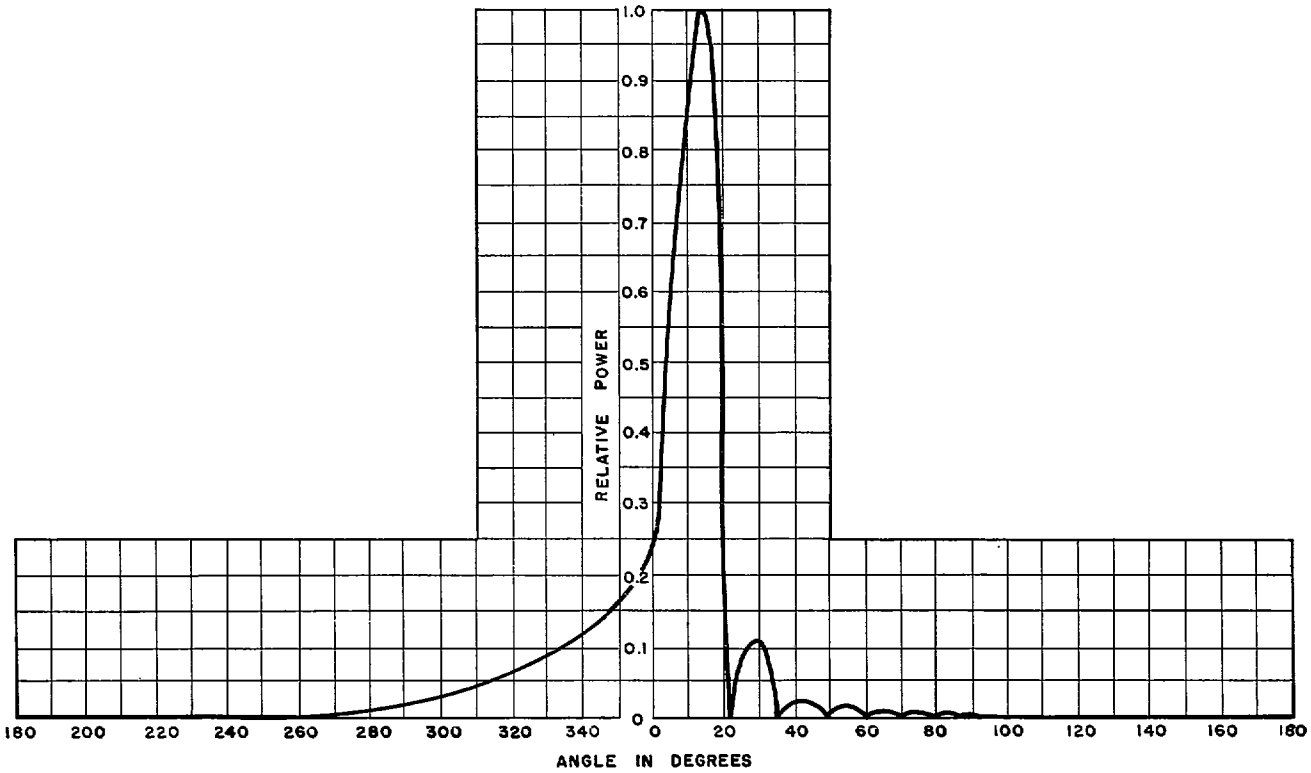


Fig. 10—Empirical radiation pattern for a 7.33λ corrugated surface with a λ/2 ground plane.

only tilts down closer to the plane, but the beamwidth narrows, approaching the infinite plane value as a limit. Plotted in Fig. 12, on following page, are the results of beamwidth measurements for a 7.33λ surface and a variety of ground planes. As can be observed, the pattern actually narrows as the endfire position is approached.

A lower bound on the beamwidth can thus be found from (31). A plot of this lower bound as a function of $1/\lambda$ is shown in Fig. 13 for $(\beta_o^s - k)l = \pi$ on the following page.

### The Effect of Finite Tooth Width

We have already observed that unless the teeth are extremely narrow, the dominant mode cannot adequately satisfy (16) and (17) and that the wider the teeth, the more the higher order modes are excited. Referring to (4), if there are twenty corrugations per wavelength,

$$\frac{\beta_1}{k} \cong 21, \quad \frac{\beta_2}{k} \cong 41, \quad \text{etc.} \tag{48}$$

and if these modes are excited, they will have radiation patterns expressed in the form of (39), with appropriate substitutions for $\alpha$, $\beta$, and $A$. The factor

$$(\alpha_n^s + jk \sin \theta) \tag{49}$$

is practically insensitive to $\theta$. The factor

$$\frac{\sin \frac{\pi l}{\lambda}\left[\frac{\beta_n^s}{k} - \cos\theta\right]}{\frac{\pi l}{\lambda}\cdot\left[\frac{\beta_n^s}{k} - \cos\theta\right]} \tag{50}$$

gives essentially the same pattern for all higher modes, i.e., $2l/\lambda$ equal lobes with the nulls occurring at different angles for different modes. The fields of these higher modes will have phase relationships which depend on the complex constants $A_n$.

An effort was made to excite these modes by constructing a corrugated surface with twenty teeth per wavelength and teeth three times as wide as the gaps. Its radiation pattern was compared with that of a similar surface in which the gaps were three times as wide as the teeth. The slot depths of the two surfaces differed by the amount necessary to establish the same value of $\beta_o^s/k$, a value chosen to satisfy the Hansen-Woodyard relation. Two typical patterns are shown for comparison in Fig. 11. No essential differences were observed. Though not reported here, this experiment was performed over a range of frequencies, for several ground plane lengths, including an effectively "infinite" ground plane, and for tooth width/gap width ratios of 3:1, 1:1, and 1:3. In no case were there any significant differences in the patterns. The conclusion appears that the higher order modes are excited when the teeth are wide but that their amplitudes are comparable and phases random so that their net effect on the radiation pattern is small.

It should be emphasized that this does not mean that the effect of the presence of higher order modes is negligible when the corrugated surface is being used as a transmission line. In that case, the impedance concept is vastly complicated by their presence and it would seem advisable to use narrow teeth in an effort to obtain an uncontaminated dominant mode.

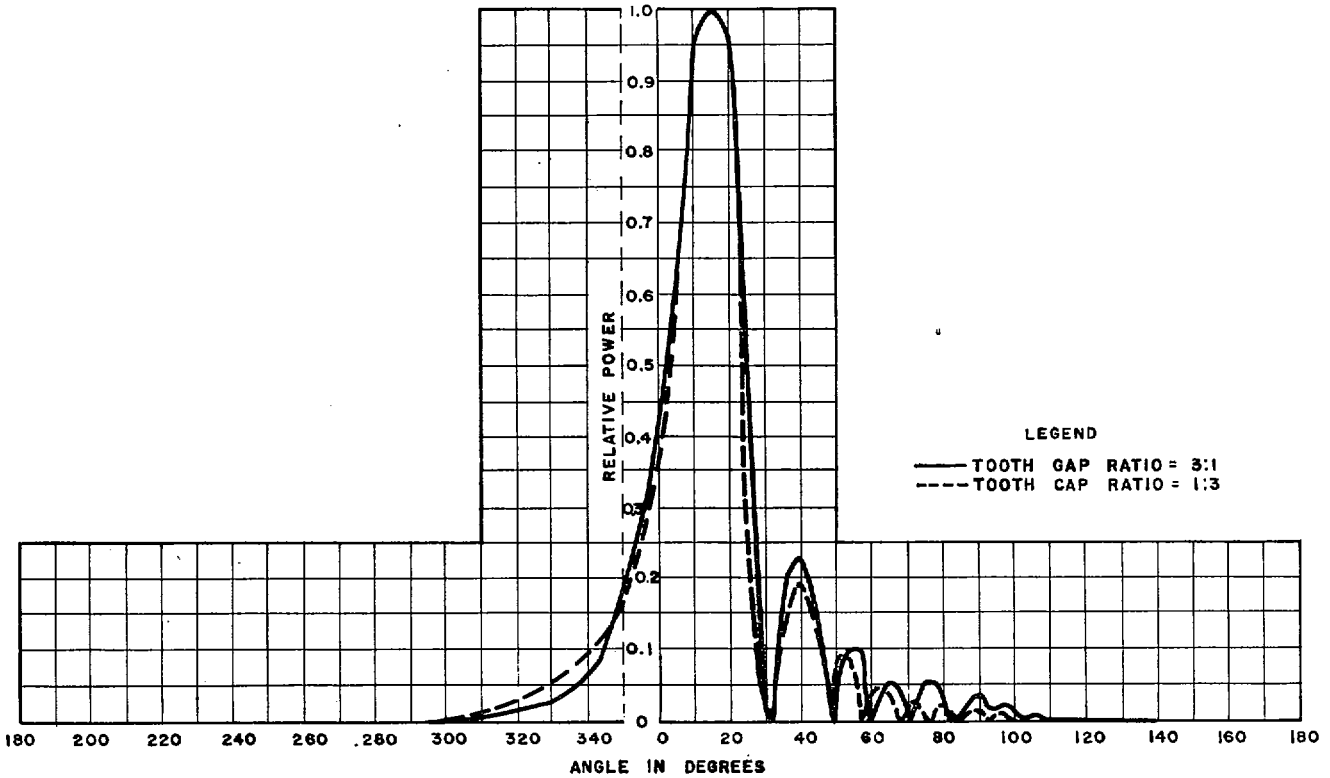


Fig. 11—Experimental radiation patterns for two corrugated surfaces 7.33λ long, one having a tooth to gap ratio of 3:1 and the other a tooth to gap ratio of 1:3, each terminated by a λ/2 ground plane.

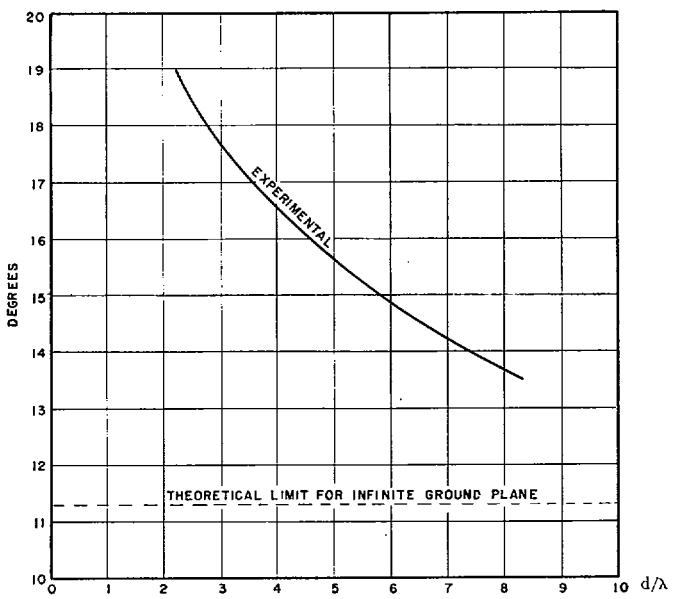


Fig. 12—Beamwidth versus ground plane length for a 7.33λ corrugated surface.

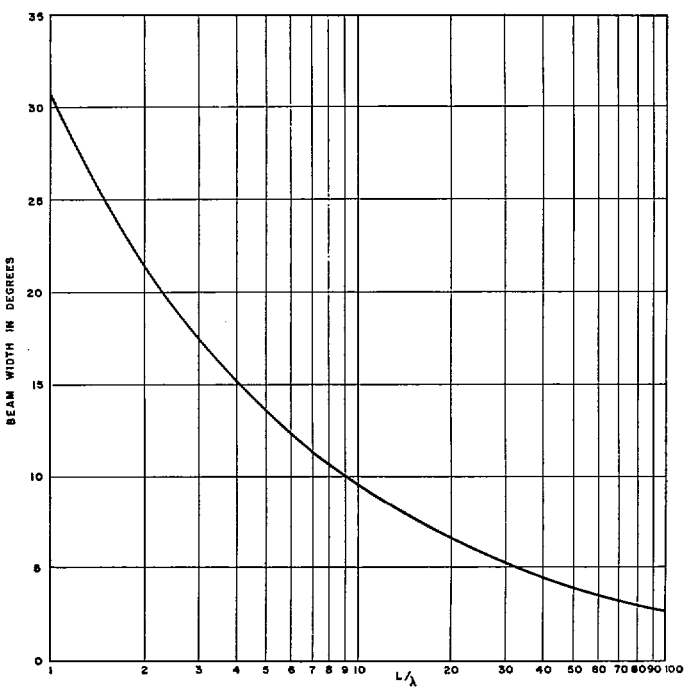


Fig. 13—Theoretical lower bound on beamwidth as a function of length of corrugated surface when Hansen-Woodyard relation is obeyed.

## Conclusions

The analysis of a flat corrugated surface appears to be strengthened by a Floquet-Lucke method of field determination. Consideration of feed radiation gives better correlation between theory and experiment. Effect of a finite ground plane can be explained approximately by classic assumption of current distribution. Effect of finite tooth width, though it complicates transmission line analysis, apparently has no influence on radiation pattern when corrugated surface is used as an antenna.

## Acknowledgment

The author is indebted to I. K. Williams for many stimulating discussions, Mrs. A. Cordova who did most of the computations, and E. N. Rodda who assisted in the experiments and the preparation of this report.